Astron. Astrophys. 271, 574–586 (1993)

ASTRONOMY AND ASTROPHYSICS

The fine structure of a chromospheric rosette

G. Tsiropoula[1], C. E. Alissandrakis[2], and B. Schmieder[3]

[1] Institute of Space Research, National Observatory of Athens, P.O. Box 20048, GR-11810 Athens, Greece
[2] Section of Astrophysics, Astronomy and Mechanics, Department of Physics, University of Athens, GR-15784 Athens, Greece
[3] Observatoire de Paris, Section d'Astrophysique de Meudon, F-92195 Meudon Principal Cedex, France

Received July 30, accepted December 4, 1992

Abstract. We have studied the spatial behaviour of the physical properties of dark mottles forming a well-defined rosette. The observations were obtained with the Multichannel Subtractive Double Pass (MSDP) spectrograph, operating in Hα at the Pic du Midi Observatory. From these observations, intensity fluctuations and Doppler shift velocities at different wavelengths were derived over a two dimensional field of view. The observed contrast profiles were matched with theoretical contrast profiles using Beckers' cloud model and 4 parameters were derived for the dark mottles: the source function, the line-of-sight velocity, the Doppler width and the optical depth. From these parameters a range for the temperature and electron density can be derived using Vernazza's et al. (1981) model D. We detected strong downflows at the roots of the mottles, while their upper part is ascending with velocities sometimes greater than 10 km s^{-1}. The values of the cloud parameters are consistent with values given by other authors for this kind of features. Consistency was also found between cloud parameters and the values given for spicules, leading to the conclusion for the identity of these structures.

Key words: lines: profile – sun: chromosphere

1. Introduction

The solar chromosphere, when seen in high quality spectroheliograms, shows a complex pattern of bright and dark fine structures, whose morphology depends strongly on the spectral line, the wavelength within the line and the position on the disk.

Quantitative information on the chromospheric inhomogeneous structure has been derived from disk observations in the EUV and in the millimetric and centimetric radio wavelengths, as well as from disk and limb observations in the visible. Foukal (1971) argued that there is a continuous morphological progression in the fine structure of the quiet and active chromosphere. Thus, features like mottles, fibrils, threads and active region filaments represent material injected into different flux tubes, the various inclinations of the local magnetic field being the most likely controlling factor. Among these structures mottles seem to be closer to the vertical flux tubes covering a large portion of the chromosphere and owe their geometry and dynamism to the existence of the magnetic field, distributed on a fine scale. These jet-like structures with characteristic widths < 1000 km and lengths between 5000 and 10000 km are distributed over the whole solar disk, but not randomly; they are mostly rising out of the chromospheric network boundaries, along magnetic flux tubes. They are dark against the disk when observed in the wings of Hα and especially enhanced in contrast at Hα ± 0.5 Å. Near the centre of the Hα line they are much less distinct. However, even such basic considerations as whether dark and bright mottles are the same feature seen at different heights or not, are still unanswered. Some authors suggest that bright and dark mottles are distinctly different phenomena (Bray 1969; Alissandrakis & Macris 1972), whereas others claim that a bright mottle is the base of a dark elongated one (Banos & Macris 1970; Dunn 1974). There is, however, general agreement that bright mottles are situated at a lower height than dark mottles and that bright and dark mottles occur in the same regions of the solar chromosphere.

Another long standing controversy exists as to whether spicules are seen against the disk at the centre of Hα as dark or bright mottles (Beckers 1968; Bray & Loughhead 1974; Athay 1976). Direct evidence for the identification of the disk counterpart of the limb spicule does not exist for various observational reasons. However, there is indirect evidence that supports the view that spicules and dark mottles constitute the limb and disk manifestation respectively of the same chromospheric structure. In terms of their geometrical distribution, lifetimes and such spectroscopic properties as source function, Doppler width and optical depth, there are similarities that suggest the identity of these structures (see Table XXV of Beckers 1968). The difference in the value of the upward velocity, which for the mottles takes the value of 6 km s^{-1} while for the spicules reaches the value of 25 - 30 km s^{-1}, can easily be interpreted provided that

Send offprint requests to: G. Tsiropoula

account is taken of the known inclinations of the spicules to the vertical.

The fine mottles usually cluster into small groups, which are called chains and larger groups, which are called rosettes (Beckers 1963). In a chain all the fine mottles point in the same direction. Seen near the limb, they all point out forming what Cragg et al. (1963) called bushes. Rosettes are the most characteristic of the various mottle groupings. They have a more or less circular form with a central bright core, which is surrounded by a number of bright and dark mottles aligned radially outwards. This non random mottle arrangement cannot be thought to be an accidental phenomenon; it is clear that it has a fundamental physical significance. Although we have not conclusive proof, a rosette might be regarded as an active region seen in microcosm, differing from the latter in scale and complexity but having the same physical origin, which is the magnetic field. This suggestion is supported by the fact that rosettes tend to be located at the vertices of the supergranulation network, where the field strength is much higher than inside the network (Frazier 1970). The total magnetic flux in the bright core of a rosette is found to be $\sim 10^{20}$ Mx (Dara-Papamargaritis & Koutchmy 1983), which is comparable to that of a pore.

The developments of the past years have emphasized that mottles are the major component of the chromospheric fine structure. Accordingly, the investigation of their physical properties is an essential step in the understanding of the quiet chromosphere. In this study we exploit the advantage of the Multichannel Subtractive Double Pass (MSDP) spectrograph (Mein 1977) in providing high resolution two dimensional images of a rosette at different wavelengths within the Hα line.

2. Observations and data reduction

The present Hα observations were performed with the MSDP (Mein 1977), operating on the solar spectrograph installed at the focus of the 50 cm refractor of the Pic du Midi Observatory on June 17, 1986 at the disk centre (N5, W5). This system, having 11 channels, allows us to observe the same point on the Sun (with coordinates x, y) simultaneously, but at a different wavelength in each channel. Thus at every point of the field of view the profile of the line can be reconstructed from 11 values. The wavelength varies within each channel along the y axis by 0.008Å per arcsec, while the shift between two successive channels is 0.256 Å. The performance of the instrument yields a contiguous $233'' \times 29''$ field of view every minute. Thus a final map ($\sim 4' \times 5.5'$) is built up from several elementary images every minute in order to cover a large region.

The duration of the present observations was 15 min. Although the spatial resolution was better than $0.5''$ the spectral resolution was relatively low, giving uncertainties of the order of 10% in intensity and about 0.5 km s^{-1} in velocity. The observations were digitized with the fast microdensitometer of the Observatory of Paris (MAMA) using a slit size of 30 μ and a step of 30 μ ($0.17''$) in both directions. The film densities were transformed into relative intensities using calibration curves deduced from profiles (David 1961). The line profiles were determined from the measured values of the intensity at the 11 points (one point by channel) and a 3rd degree spline interpolation was used in order to reconstruct the entire line profile for each pixel of the field of view. Thus the processed MSDP spectra can provide two dimensional intensity and velocity maps at several depths in the line. An average profile was obtained for each position y, by averaging the profile over quiet regions along the large dimension of the field of view.

For the computation of the line of sight velocity we found the point in the profile where the half width is $\Delta\lambda$ (0.256, 0.512, 0.768 Å), both for the average profile and for the profile at each pixel. The wavelength shift of each chord with respect to the average profile is used to compute the velocity ($V_{\pm\Delta\lambda}$), while the relative depth of the chord determines the intensity ($I_{\pm\Delta\lambda}$). Then, maps of intensity and Doppler velocities were computed from the profiles by this method simulating the "lambdameter" technique (Mein 1977). In addition, monochromatic images at +0.25Å, −0.25Å, +0.5Å, −0.5Å, +0.75Å and −0.75Å were computed simulating filtergram technique.

From the entire sequence one frame of very good quality was selected in order to study physical parameters and their statistical properties in mottles forming a very well defined rosette.

3. Method of computation

The disk observations of the chromospheric fine structure reveal a pattern of bright and dark features, whose appearance is due to the variation of the emerging radiation intensity, $I(\lambda)$. The determination of physical quantities from these disturbed intensity profiles is essential in extending our incomplete information on the physical processes responsible for the observed patterns. However, the problem of derivation of fully consistent models, that will correctly describe the variation of the intensity in terms of the physical parameters involved, is very complicated as it needs multi-dimensional solutions of the non-LTE transfer equations and is far from being solved.

A rather convenient way of extracting information from a large amount of Hα observations is by studying the contrast of the features as a function of the wavelength, in terms of Beckers' cloud model (Beckers 1964). This model has been used extensively in the analysis of chromospheric features seen in the Balmer lines (Grossmann-Doerth & von Uexküll 1971, 1973, 1977; Bray 1973, 1974; Bray & Loughhead 1983; Alissandrakis et al. 1990; Tsiropoula et al. 1991). The cloud model considers the feature as a "cloud" overlying a uniform atmosphere and, assuming that the source function S is frequency independent and constant throughout the cloud, adopts a four parameter representation of the contrast profile:

$$C(\Delta\lambda) = \frac{I(\Delta\lambda) - I_o(\Delta\lambda)}{I_o(\Delta\lambda)} = \left(\frac{S}{I_o(\Delta\lambda)} - 1\right)\left(1 - e^{-\tau(\Delta\lambda)}\right)$$

where $I_o(\Delta\lambda)$ is the reference profile emitted by the background. In addition, one assumes that the optical thickness has a gaussian form:

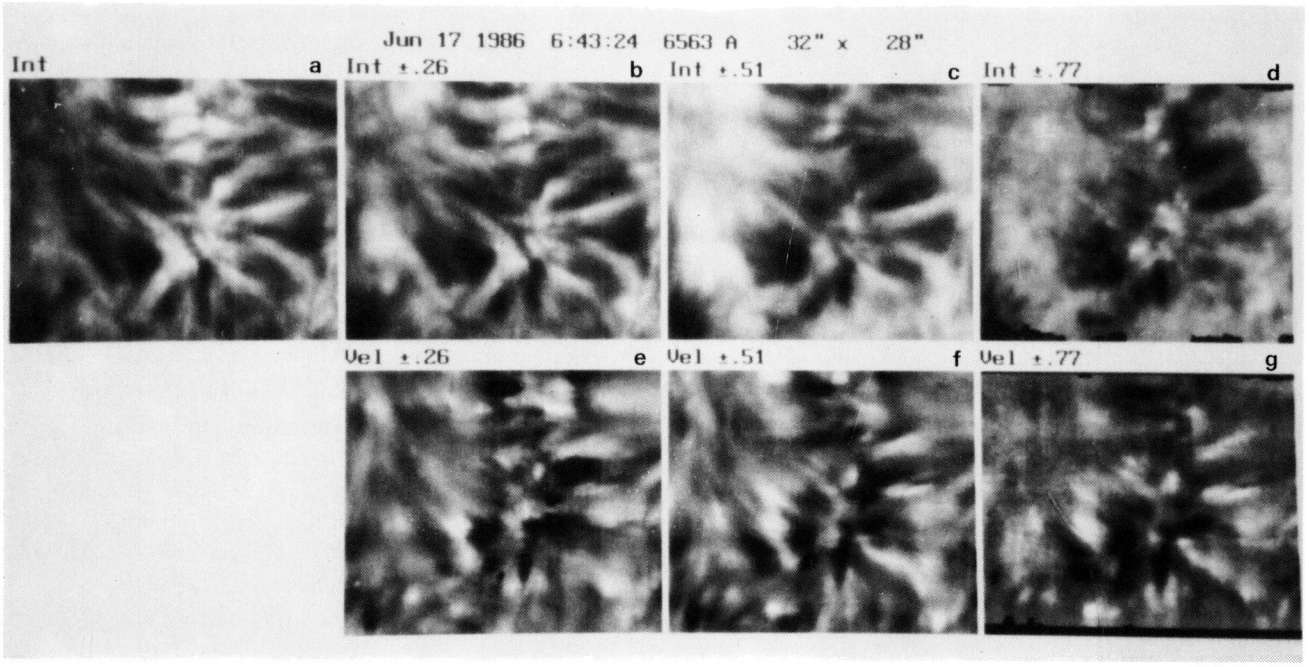

Fig. 1. Computed intensities and Doppler velocities of a chromospheric rosette at different wavelengths of the Hα line at N5W5 observed from the Pic du Midi Observatory on June 17, 1986

$$\tau(\Delta\lambda) = \tau_o e^{-(\frac{\Delta\lambda-\Delta\lambda_I}{\Delta\lambda_D})^2}$$

and that the optical depth τ_0, the Doppler shift $\Delta\lambda_I$, and the Doppler width $\Delta\lambda_D$, are constant throughout the cloud. Thus, this model permits to derive several physical parameters of the elements of the chromospheric fine structure. However, as has already been pointed out (Alissandrakis et al. 1990), only under a restricted range of circumstances can this model account in a physically consistent way for the observed contrasts. The most basic of these is that only structural elements lying at such a height that the Hα line is entirely formed below their lower boundary can be matched by this model. Dark mottles, having heights of at least 5000 – 7000 km above the base of the chromosphere (Beckers 1968; Bray & Loughhead 1974), are suitable for the application of the cloud model. On the other hand, bright mottles are "low" clouds since they lie at heights less than 3300 km and have contrast profiles that cannot be matched by this model.

Another common and widely used method to measure line of sight velocities is by determining the Doppler shift of a spectral line and from this the line of sight velocity. The determination of the velocities in this way is valid if the moving structure is located low enough so that the observed profile is formed entirely within the structure (Bray & Loughhead 1973; Bray 1974; Durrant 1975; Steinitz et al. 1977). This is not true for the dark mottles which are "high" clouds. In this case the Doppler shift method gives line of sight velocities systematically lower than the cloud velocities. However, as pointed out by Alissandrakis et al. (1990), the general behaviour of the velocities obtained from these two methods is exactly the same, e.g. positive or negative velocities are found in the same place. Thus the results of this method can be used for a qualitative description of the velocity pattern of a region.

The computation of the four parameters of the cloud model was carried out by an iterative least square procedure for non linear functions, taking into account the restrictions described in Alissandrakis et al. (1990).

4. Results

4.1. Morphology at different wavelengths

The rosette under study had a size of 22″ by 25″ and consisted of fine mottles whose roots formed a circular pattern while their opposite ends diverged in all directions (Fig. 1). Some mottles were round and some elongated; they had an horizontal extent of 4 to 6″ a width of 1.7 to 3″ and most of them appear to consist of finer structures, unresolved at the line centre but resolved in the far wings.

Let us consider the appearance of the mottles when observed at different wavelengths. At the Hα line center (Fig. 1a) the bright and dark mottles form a pattern which is somewhat confusing. Individual bright mottles occupy the space between dark mottles, are less numerous and cover a smaller area. The central region appears bright and it is overlaid by some dark structures which appear to be more or less horizontal.

The pattern becomes less confusing as one moves out into the wings of the Hα line. At Hα ±0.256Å (Fig. 1b) there is a little difference: dark mottles become more distinct, while bright mottles lose contrast. Dark mottles show noticeable changes at Hα ±0.512Å (Fig. 1c); most mottles are elongated, extend

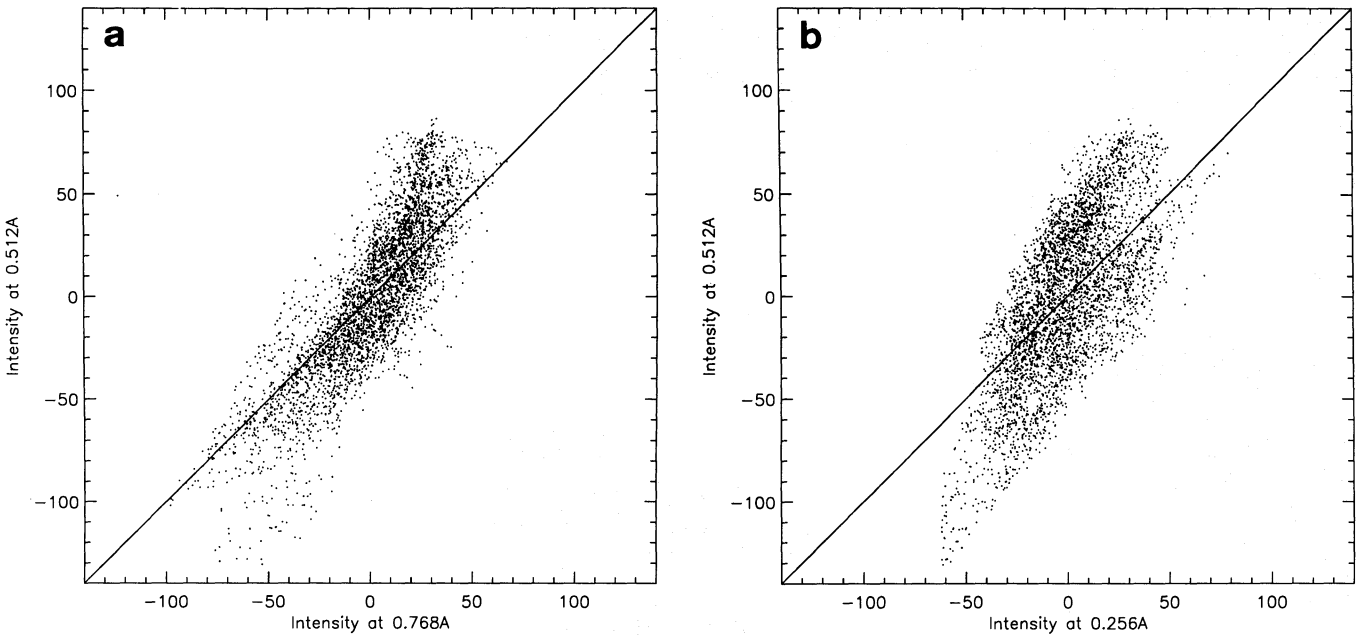

Fig. 2. a, b Correlation diagrams of Hα intensity. **a** $I_{\pm 0.512}$ versus $I_{\pm 0.768}$. **b** $I_{\pm 0.512}$ versus $I_{\pm 0.256}$

from the central region of the rosette and gradually fade out. They attain their maximum visibility at this wavelength and it becomes easier to distinguish individual mottles. This is due to the fact that dark mottles have line profiles broader than the average Hα profile (cf section 4.3). The correlation diagrams of the intensities $I_{\pm 0.512}$ versus $I_{\pm 0.768}$ (Fig. 2a) and $I_{\pm 0.512}$ versus $I_{\pm 0.256}$ (Fig. 2b) show that bright pixels are in general brighter at Hα ±0.512Å than at Hα ±0.256Å and Hα ±0.768Å while dark pixels are darker at Hα ±0.512Å than at the two other wavelengths.

At Hα ±0.768Å (Fig. 1d) some dark mottles are no more visible, while those that are visible appear more elongated and their apparent sizes are reduced. This can be explained by the argument that as one moves out into the far wings the optical thickness drops and therefore some structures become transparent, which results in zero contrast. Bright mottles are no longer visible at these wavelengths. We can notice, however, that the more prominent dark mottles visible in the wings are also distinguishable at the line centre. In the Hα ±0.768Å map (Fig. 1d) chain-like bright features can be identified at the centre of the rosette. These features, which Dunn & Zirker (1973) named filigree, appear at the boundaries of the supergranules and are thought to be closely associated with small scale magnetic fields, of kilogauss strength. Their brightness, however, provides no information about the magnetic polarity, which is highly desirable if we want to clarify whether bipolar fields exist on a fine scale in the network.

Fig. 3 shows computed images on opposite wings of the Hα line, simulating observations taken with monochromatic filters. Comparing the images at different wavelengths on the same wing of the line, we find a close agreement in the size, shape and location of individual mottles, although the contrast varies, being maximum at ±0.50Å. The comparison of images on opposite wings shows no detailed agreement, especially in the size. At the same distance from the line centre the dark mottles appear to be more contrasted in the blue wing than in the red (except at Hα −0.75Å, where they are very reduced in size), while the rosette gives the impression of containing more dark mottles in the red wing than in the blue. Dark mottles appear to penetrate somewhat further towards the centre of the rosette and appear coarser in the red wing than at the blue wing. At the centre of the rosette the filigree can be identified not only at Hα −0.75Å, but also at Hα −0.5Å.

4.2. Doppler velocities at different wavelengths

Fig. 1f, 1g and 1h show maps of Doppler velocities at ±0.256Å, ±0.512Å and ±0.768Å respectively. As the rosette is located near the disk center, these velocities correspond to vertical material motions. A contour map of the Doppler velocity at ±0.512Å is given in Fig. 4. On a large scale the velocity is positive (ascending) near the center of the rosette, within a circle of $\sim 2''$ radius; between $\sim 2''$ and $\sim 7''$ it is predominantly negative (descending) and becomes again positive further away. Downflows seem to occur in bright mottles and at the roots of the dark mottles, while their upper parts are ascending at all wavelengths. There are, however, cases where the entire dark mottle shows ascending motions (upper right part of the rosette, Fig. 1) as well as one case of apparent ascending motions at the middle of the mottles and descending motions at both edges. This last remark refers to a bunch of mottles in the lower left part of the rosette and reminds of motions associated with rising magnetic flux tubes in Arch Filament Systems.

The limits of the dark and bright mottles in the intensity maps of Fig. 1 do not coincide with the limits of velocity struc-

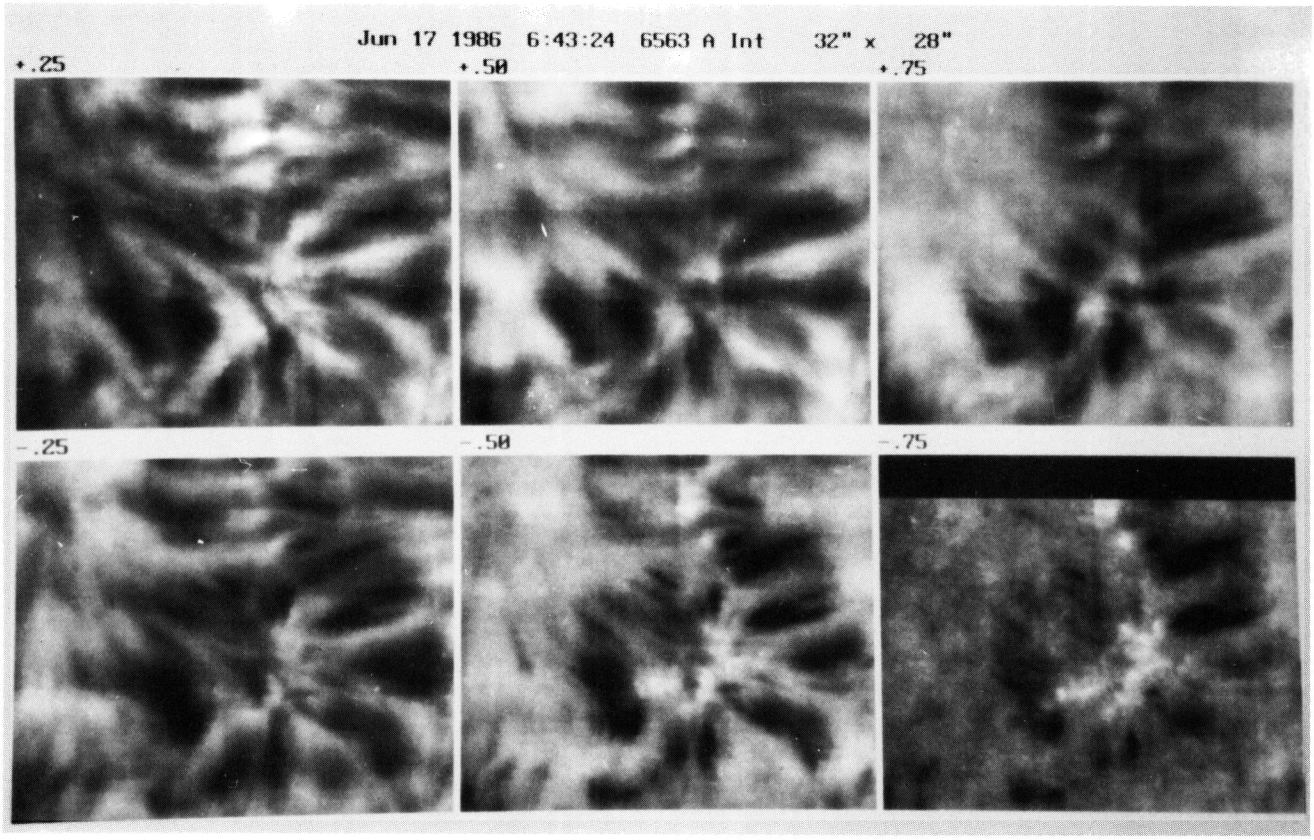

Fig. 3. Computed intensities of the rosette region on opposite sides of the Hα line and at equal intervals from the line centre

tures in the Doppler maps. This suggests that bright and dark mottles are parts of same structures, but having different physical conditions. However, the dark mottles visible in the blue wing of Hα (Fig. 3c) and those visible in the red wing (Fig. 3b) coincide with blue and red shifted features in the velocity maps of Fig. 1.

The velocities $V_{\pm 0.512}$ and $V_{\pm 0.768}$ are well correlated (Fig. 5a), while the velocities measured at Hα ± 0.512 are in general smaller by a factor of 2 compared to the velocities measured at Hα ± 0.256 Å (Fig. 5b). The velocity dispersion is greater for the dark pixels than for the bright pixels. This can easily be seen in the histograms of Fig. 6. Thus at ± 0.512Å bright pixels have a velocity dispersion of ± 2.5 km s^{-1}, (Fig. 6a), while the dispersion for dark pixels is between -5 to 3 km s^{-1} (Fig. 6b).

Table 1. Parameters of dark mottles derived with the cloud model

Parameter	Average value	Standard deviation
Source function	163.3	14.3
Velocity (km s^{-1})	-0.26	6.6
Optical depth	1.8	1.1
Doppler width (Å)	0.37	0.1

4.3. Hα profiles

The study of line profiles gives a better insight than mere intensity and Doppler shift maps. Four such profiles are given in Fig. 7, together with the average Hα profile. Figure 7a shows a bright mottle profile which is bright near the core of Hα and very near the background intensity everywhere else. However, many bright mottle profiles are broader than the background profile and shifted towards the blue or the red, as the one shown in Fig. 7b. Such wide profiles explain why some mottles which are bright at the center of Hα appear dark at 0.512 Å.

The dark mottles show a large broadening on both wings of the line (Fig. 7c) or, sometimes, on one wing only (Fig. 7d). Such profiles could be interpreted as the sum of profiles of different structures with different line of sight velocities, or in terms of turbulent velocities or a velocity gradient (Athay 1970).

For the broadened profiles of dark mottles, more realistic values for the velocity are derived by using the cloud model; thus for the profile of fig. 7c the cloud model gives -11.3 km s^{-1}, while the standard method gives only -3.2 km s^{-1} which is actually a lower limit since it averages the velocity of the moving feature and the stationary background. On the contrary, non-LTE computations would be necessary in order to obtain a better estimate of the velocity than the one given by the direct measurement of the Doppler shift.

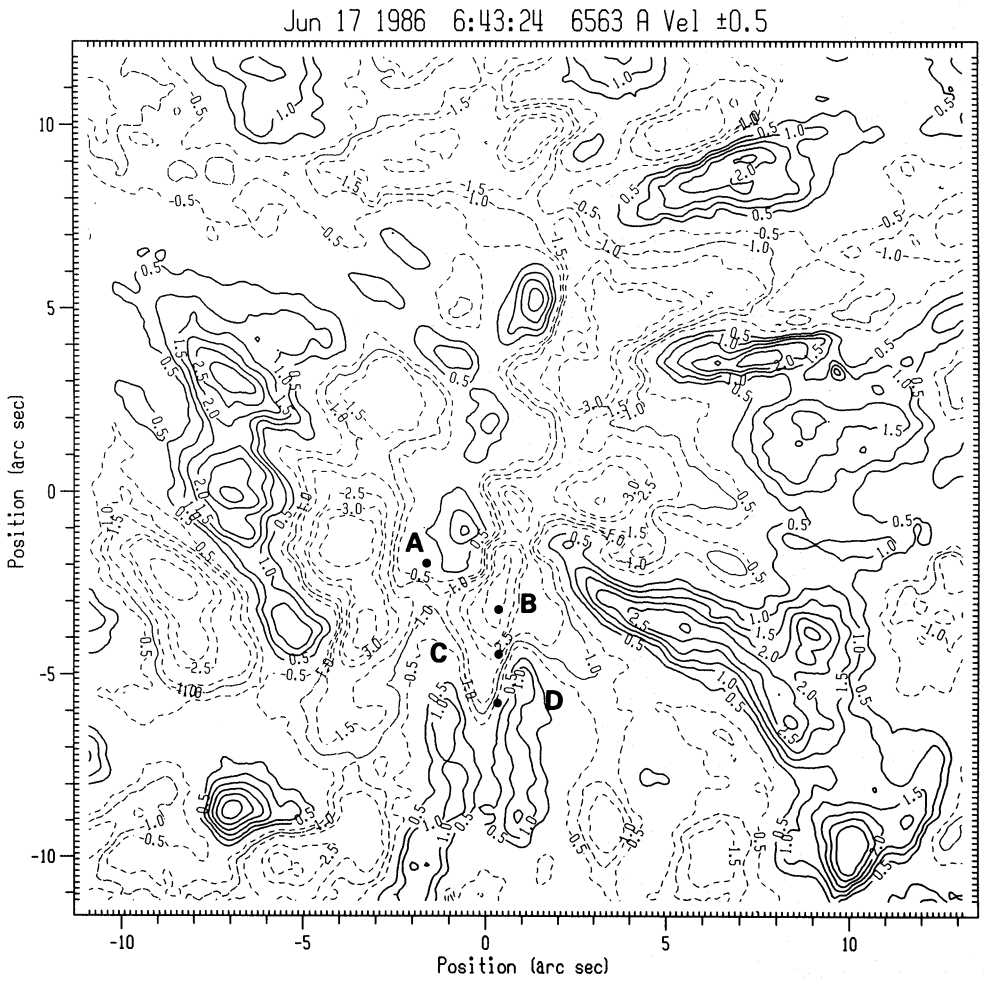

Fig. 4. Contour map of the velocity in the rosette region obtained with the Doppler shift method at ±0.512Å

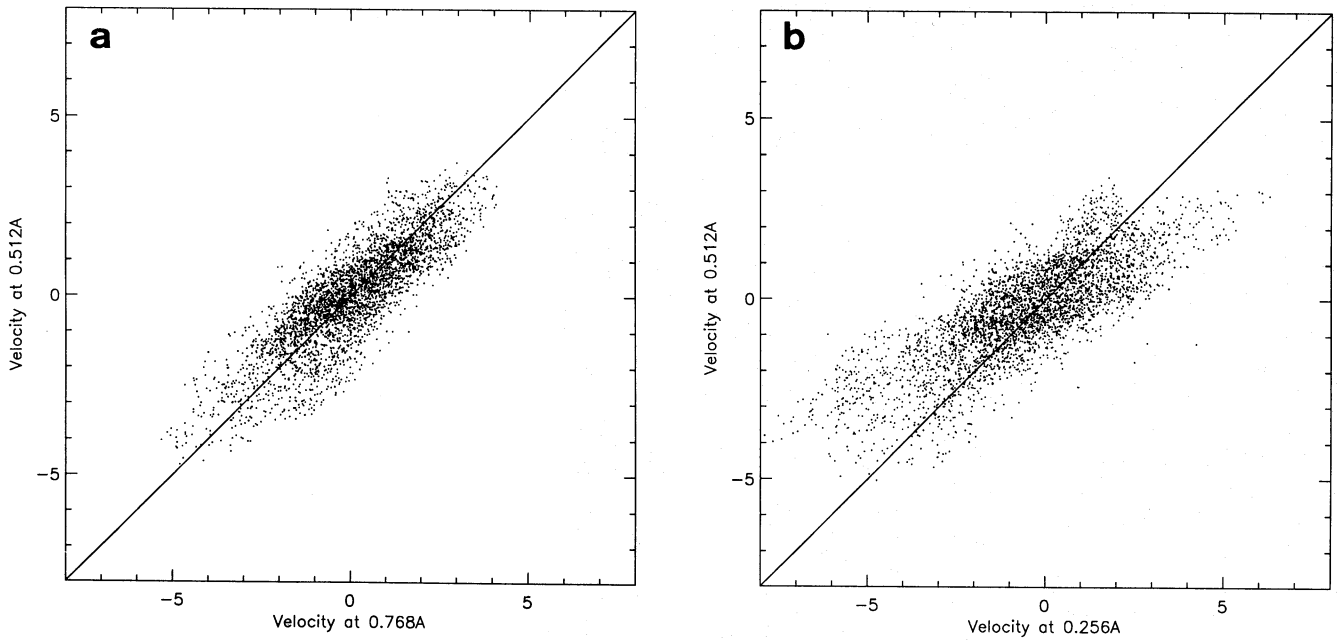

Fig. 5. a, b Correlation diagrams of Doppler velocities. **a** $V_{\pm 0.512}$ versus $V_{\pm 0.768}$. **b** $V_{\pm 0.512}$ versus $V_{\pm 0.256}$

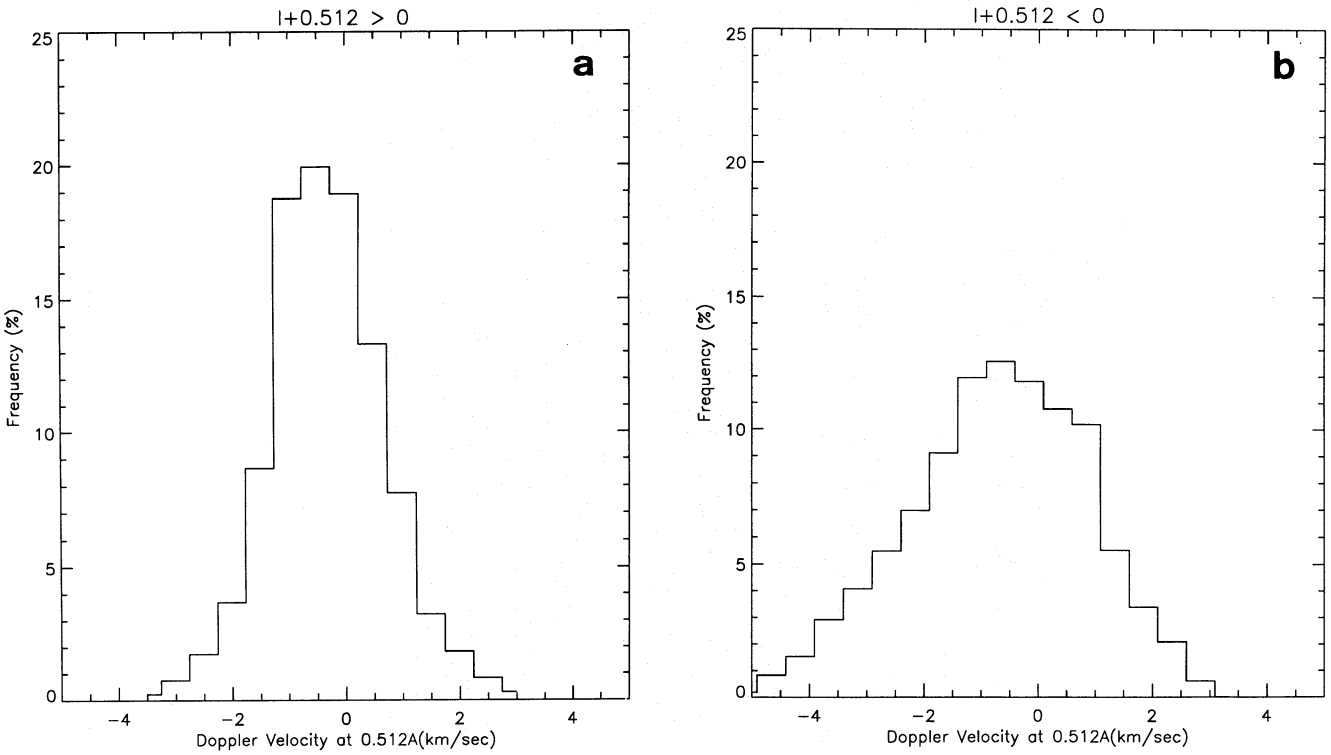

Fig. 6. a, b Histograms of Doppler velocities at ±0.512Å. **a** For $I_{\pm 0.512} > 0$ (bright pixels). **b** For $I_{\pm 0.512} < 0$ (dark pixels)

4.4. Cloud model parameters for dark mottles

About 6000 out of 22500 pixels, whose profiles satisfied the cloud model criteria were treated; these were primarily dark pixels which have absolute contrast profiles less than about 0.1 throughout the line (Alissandrakis et al. 1990). We emphasize that, in physical terms, the difference between brightness and darkness of a mottle translates to a difference between source function values, the value of the source function being smaller than the background intensity at line centre in the high (dark) mottles and greater than the intensity at all wavelengths in the low (bright) mottles. This difference should be interpreted by an appropriate non-LTE theory in terms of such quantities as temperature and electron density. Thus, contrast profiles of bright mottles cannot be matched by the cloud model. Table 1 gives the average value and standard deviation of each parameter derived with the cloud model for dark mottles.

Fig. 8a shows the map of the source function; it has a smooth variation with a minimum value of 150-160 (in units of 1/1000 of the continuum intensity) near the axis of individual mottles and exceeds the value of the background intensity (~170) near the edge. These latter values should be treated with some caution, because of the requirements for the validity of the cloud model (Alissandrakis et al. 1990); therefore only pixels with source function less than 180 were used for the histograms, the values given in Table 1 and the scatter plots in this work. The histogram of the source function (Fig. 9a) peaks around 170, with some values as low as 100 and a mean value of 163. Fig. 8b shows the map of the line of sight velocity. As in the case of the Doppler velocity of Fig. 4, downflows occur predominantly in the inner part of the rosette and upflows in the outer part, with velocities sometimes greater than 10 km s^{-1}. This is in contradiction with the general accepted view which was a problem for the identification of dark mottles with spicules e.g. that dark mottles have line of sight velocities which are not as large as the limb observations would require. Grossmann-Doerth & von Uexküll (1973) must be correct in believing that this effect was a consequence of the existing inability to resolve structures with a spatial resolution better than 1″.

The velocity histogram (Fig. 9b) is rather asymmetric (cf Fig. 6b). It peaks around 1 km s^{-1} with a mean value of −0.26 km s^{-1} and individual values ranging from about −20 km s^{-1} to 20 km s^{-1}. A comparison between cloud velocities and Doppler velocities at ±0.512Å is given in Fig. 10. Cloud velocities are generally several times greater than Doppler velocities, because only a part of the line forms in the moving feature, while the deviations are greater at larger velocities than around zero. As can be seen, however, from Fig. 8b and 4 and the scatter plot of Fig. 10, the velocities found from these two different methods have the same behaviour i.e. positive or negative velocities are found at the same places.

Fig. 8c and 8d show maps of the optical depth at line centre and Doppler width. We notice that regions of high optical depth have low Doppler width and vice versa. This is not surprising since, as it is noticed already by Alissandrakis et al. (1990), there is an anticorrelation for given N_2 and L between τ_o and $\Delta\lambda_D$, i. e. $\tau_o \propto N_2 L/\Delta\lambda_D$, where N_2 is the number density in the second hydrogen level and L is the geometrical thickness

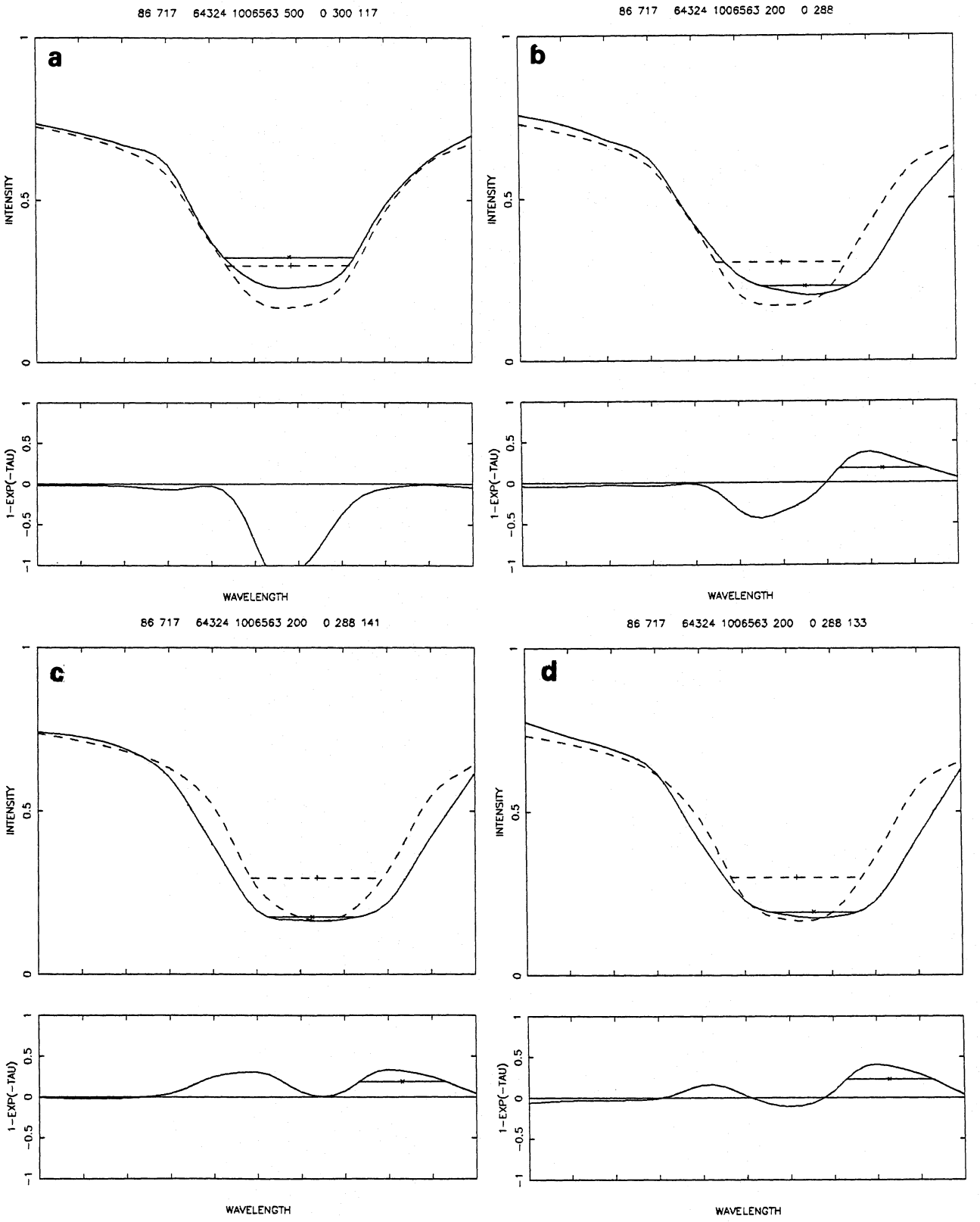

Fig. 7. a-d Hα profiles (solid line) in bright **a, b** and dark **c, d** mottles. The locations of the corresponding pixels are marked in Figs. 4 and 8. The dashed curves show the background profile

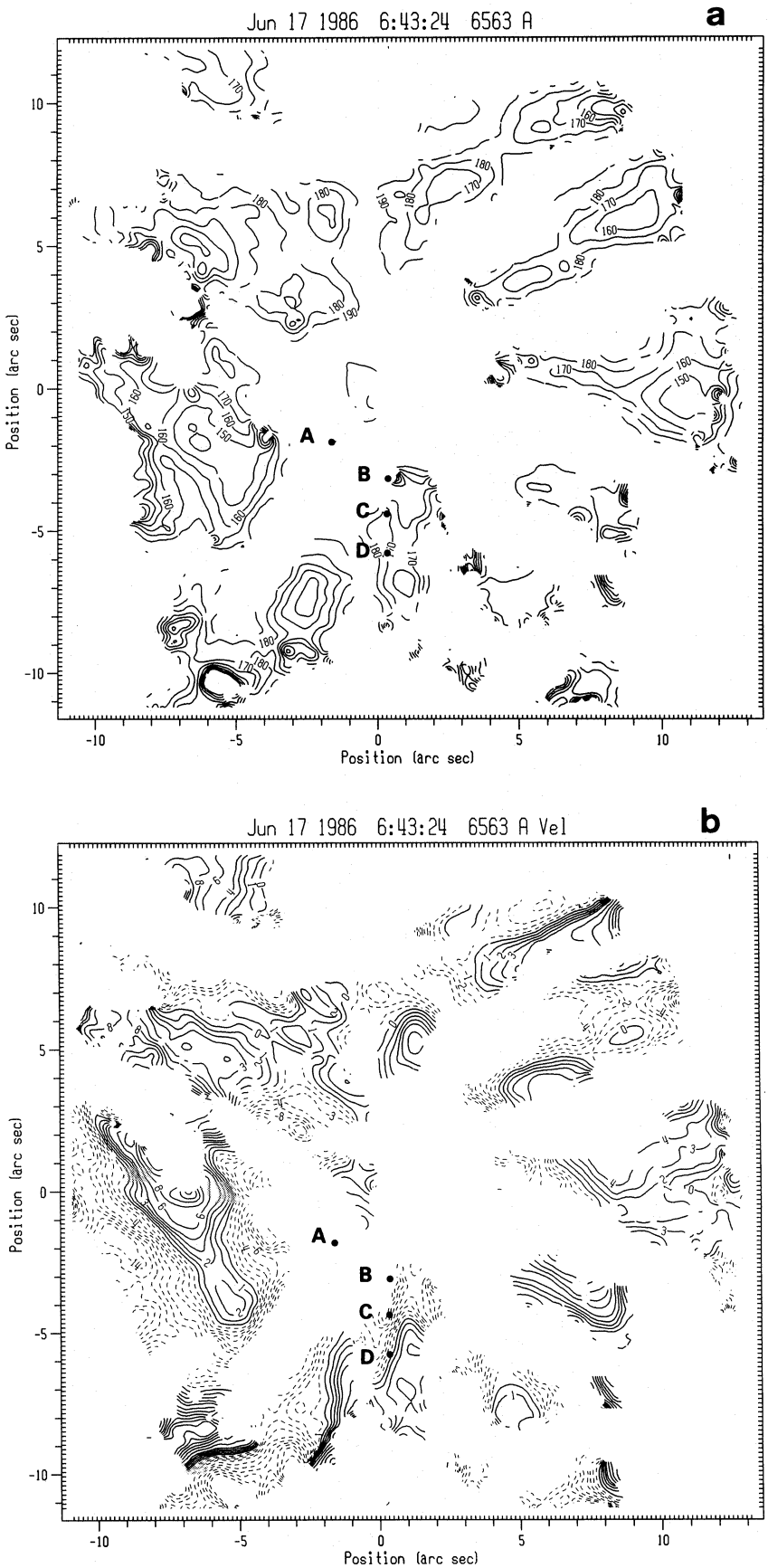

Fig. 8. a, b Parameters derived with the cloud model. **a** source function, **b** velocity

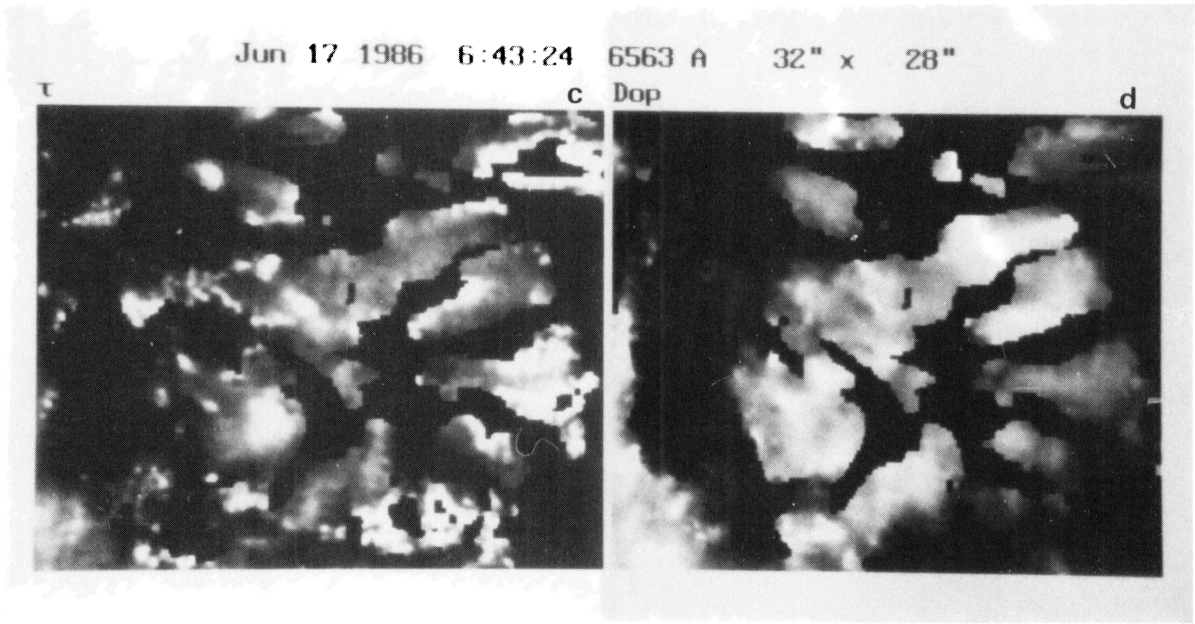

Fig. 8. (continued) **c** Optical depth and **d** Doppler width

of the mottle. Using this relation and the mean values of τ_o and $\Delta\lambda_D$ (Table 1) we can have an estimate of the quantity $N_2 L$. This is equal to 4.9 x 10^{12} cm^{-2}; L being in the range 1.1 - 2.2 x 10^8 cm, N_2 takes values in the range 2.2 - 4.4 x 10^4 cm^{-3}. Comparing this range of values with Vernazza' s et al. (1981) model D, we can arrive to a range of temperature, T, and electron density, N_e: thus the temperature seems to be in the range 7100 - 13000 K and the electron density in the range of 4 - 4.9 x 10^{10} cm^{-3}. Chou & Zirin (1988) estimated the temperature of arch filaments observed in Hα at 6000-15000 K and the total number density of hydrogen N_{tot} at $10^{11} - 10^{12}$ cm^{-3}. N_{tot} is greater than $N_1 + N_e$. We can conclude that N_e is less than this value in any case.

The values of the four parameters derived with the cloud model for the dark mottles are consistent with the values found by other authors (Table 2)

The histogram of the optical depth (Fig. 9c) peaks around 1.3 and the mean value is 1.8, suggesting that the structural elements studied are optically thin or, at least, not optically very thick. The histogram of the Doppler width (Fig. 9d) peaks around .35Å, which is near the thermal value for a temperature of 15000 K, with individual values ranging between .1Å and .65Å. Alissandrakis et al.. (1990) found that the velocity is not strongly coupled with the other three parameters. Their result confirms the theoretical result of Durrant (1975) that the computed velocity is relatively insensitive to the precise value of the source function S_0, at least the velocity values derived with the cloud model remain valid even for values of τ_0 greater than 1 (not too greater , however).

5. Discussion

A two dimensional analysis with high spatial resolution using the MSDP spectrograph in conjunction with the cloud model provides us a powerful tool for a better understanding of the physical properties of the chromospheric fine structure.

At the very center of the rosette upflows were observed. However, the predominant pattern of bulk motion in dark mottles is that of downflow at their footpoints and upflow at their tops. This can be consistent with a picture of an initial flow acceleration, where the material follows the field lines with upward motion in the first phase. The kinetic energy being not enough to push the material further up leads to a deceleration, the material at the base being the first to go down, while the other end continues going up. An analogous configuration has been proposed by Mein & Mein (1982) and by Schmieder et al. (1983) for mass ejections. Recently, Schmieder et al. (1991) observed bushes at the footpoints of a filament physically similar to rosettes in the chromospheric network with upward and downward velocities. Alternatively, this behaviour is similar to the one prediced by the model of Pikel'ner (1969), in which the magnetic field accelerates the plasma both towards the corona and towards the photosphere, in the upper and lower part of the magnetic structure respectively. However, both pictures are speculative at this time and a temporal series of observations needs to be considered.

It is interesting to note that systematic downflows have also been observed in the chromosphere-corona transition region at EUV wavelengths both in quiet and in active regions. In quiet regions these downflows of 5 km s^{-1} are correlated with the bright regions of the chromospheric network (Dere et al. 1984). At the photospheric levels strong downflows were expected in regions of concentrated magnetic field (Parker 1978) such as

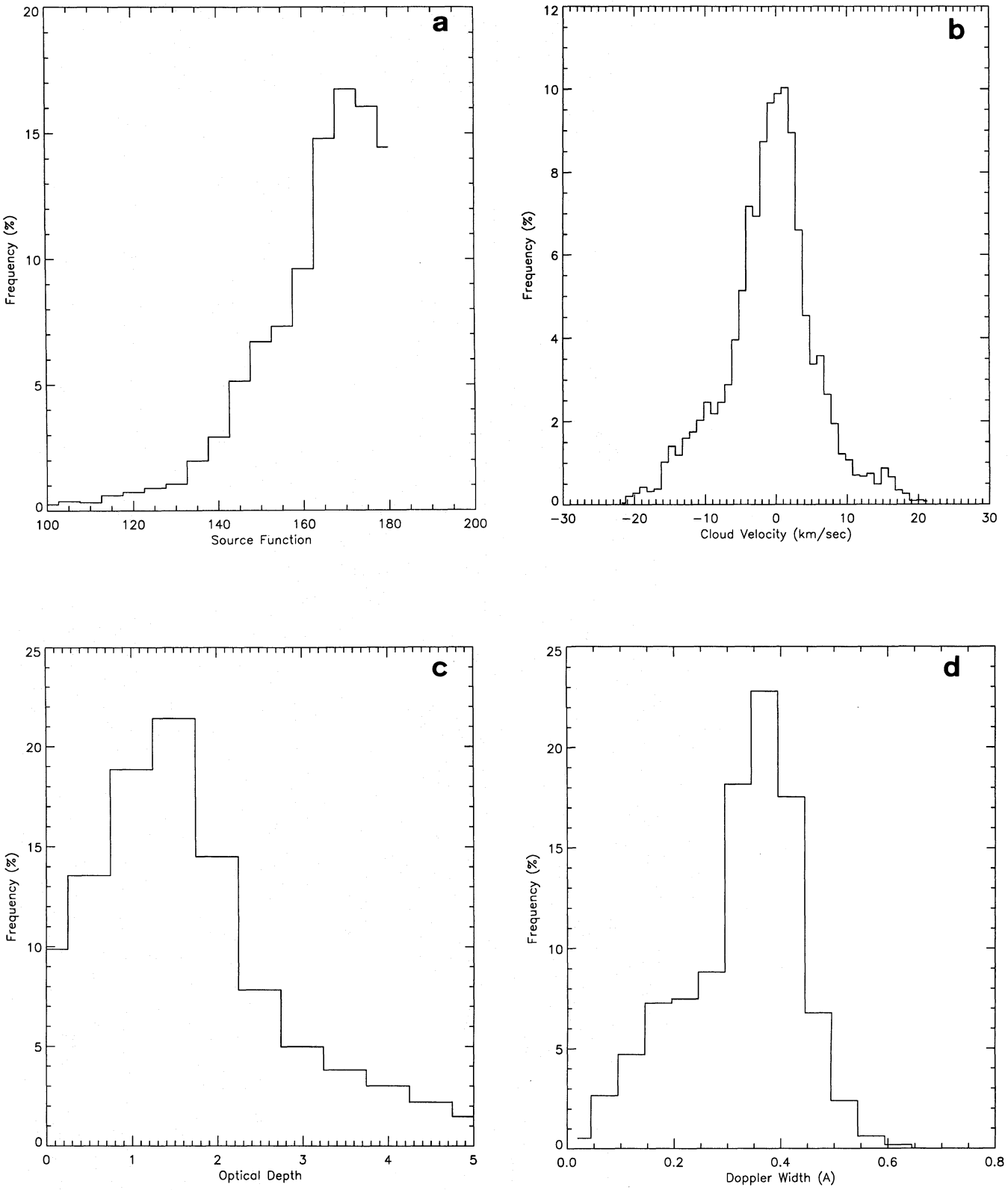

Fig. 9. a-d Histograms of the 4 parameters derived with the cloud model in the rosette region: **a** Source function, **b** Velocity, **c** Optical depth, **d** Doppler width.

Table 2. Parameters of dark mottles derived by different authors

Parameter	Beckers 1968	Bray 1973	Grossmann-Doerth & von Uexküll 1977
Source function	123	130-160	130
Velocity (km s^{-1})		−9 to +7	−8 to +8
Optical depth	1.4	1.	1.1
Doppler width (Å)	0.5	0.5	0.45

Table 3. Parameters of spicules derived by different authors

Parameters	Beckers (1968)	Alissandrakis (1973)	Krall et al. (1976)	Matsuno and Hirayama (1988)
Source function	110-190			
Optical depth	1.2-3.6	1.25-2.25		
Doppler width (Å)	0.5	0.5		
Temperature (K)	12000-16000	13000	12000-16000	5200-9000
El. density (cm^{-3})	6×10^{10}	$6 - 11 \times 10^{10}$	6×10^{10}	

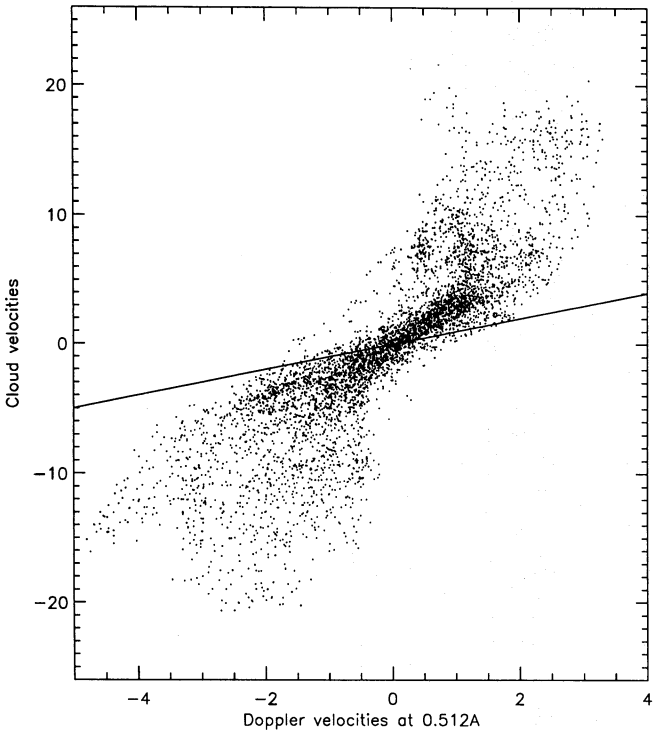

Fig. 10. Comparison of the velocities calculated with the cloud model and the Doppler velocities at ±0.512Å

rosettes. Recent observations, however, showed that the actual downflows are not much stronger than ordinary downflows associated with descending granular motions (Dara et al. 1987; Alissandrakis et al. 1991).

The important question of the identification of mottles with spicules observed beyond the limb can be answered only after a detailed consideration and intercomparison of the properties of the two features. Thus, the elongated dark mottles and limb spicules have their optimum visibility at the same wavelengths in the wings of Hα. Lifetime, height, vertical and horizontal dimensions are also in good agreement (see Table 3.3 of Bray & Loughhead 1974). Considering the values of some physical properties found for spicules by different authors (Table 3) with the corresponding values found for dark mottles one can conclude for the identity of these features. The values for the source function and the optical depth of Beckers are theoretical values given by a spicule model at a height of 5000–7000 (Beckers 1968, Table XXVI). The differences between these values and ours (Table 1 and section 4.3) may be due to the fact that these structures are observed under very different conditions: in one case (disk) at low heights and along the vertical, in the other case (limb) at great heights and along an horizontal line of sight.

A detailed comparison between the observed and theoretical profiles can enable us to unify in a comprehensive theory the dynamics, morphology and physical state of the chromospheric fine structure. There is a need for further work in order to determine the temporal and spatial variation of contrast profiles at different locations within mottles, the structures which seem to be the basic constituent of the chromosphere. It is obvious that these variations reflect changes in the magnitude and direction of the magnetic field and in the pressure density state. Thus their study would help us to elucidate the significance of the geometrical organization of these structures within the rosette pattern. Also, the mass and energy flow represented by mottles is a critical factor in the overall mass and energy balance of the chromosphere and corona.

Acknowledgements. The authors are indebted to R. Hellier and C. Coutard for the observations and to P. Mein and P.Heinzel for useful comments and discussions. Travel funds for this work were provided in part through the bilateral exchange program between France and Greece. The film was digitized by the fast microdensitometer MAMA of INSU (CNRS).

References

Alissandrakis C. E. and Macris C., 1971, Solar Phys., 20, 47
Alissandrakis C. E., 1973, Solar Phys., 32, 345
Alissandrakis C. E., Tsiropoula G., Mein P., 1990, A&A, 230, 200
Alissandrakis C. E., Dara H. C. and Koutchmy S., 1991, A&A. 249 533
Athay R. G. 1970, Solar Phys., 12, 175.
Athay R. G. 1976, The Solar Chromosphere and Corona (Dordrecht: D. Reidel Publishing Co.)
Banos G. J. and Macris, C. J., 1970, Solar Phys., 12, 106
Beckers J. M., 1963, ApJ, 138, 648
Beckers J. M., 1964, Ph. D. Thesis, Utrecht
Beckers J. M., 1968, Solar Phys., 3, 367
Beckers J. M., 1972, ARAA, 10, 73
Bray R. J., 1969, Solar Phys., 10, 63
Bray R. J., 1973, Solar Phys., 29, 317
Bray R. J., 1974, Solar Phys., 38, 377
Bray R. J. and Loughhead, R. E. 1974, The Solar Chromosphere (London: Chapman and Hall)
Bray R. J., Loughhead R. E., 1983, Solar Phys., 85, 131
Chou D.Y. and Zirin H., 1988, ApJ, 33,420
Cragg T., Howard R. and Zirin H., 1963, ApJ, 138, 303
Dara-Papamargariti H. and Koutchmy S., 1983, A&A, 125, 280
Dara H. C., Alissandrakis, C. E. and Koutchmy S., 1987, Solar Phys., 109,19
David K.H., 1961, Z. Astrophys., 53, 37
Dere K.P., Bartoe J.-D.F. and Brueckner G.E., 1984, ApJ, 281, 870
Dunn R. B. and Zirker J. B., 1973, Solar Phys., 33, 281
Dunn R. B., 1974,
Durrant C. J., 1975, Solar Phys., 44, 41
Frazier E. N., 1970, Solar Phys., 14, 89
Grossmann-Doerth U., Von Uexküll M., 1971, Solar Phys., 20, 31
Grossmann-Doerth U., Von Uexküll M., 1973, Solar Phys., 28, 319
Grossmann-Doerth U., Von Uexküll M., 1977, Solar Phys., 55, 321
Krall K.R., Bessey R.J. and Beckers J.M., 1976, Solar Phys., 46, 93
Martin S. F., 1990, Lecture Notes in Physics, (Springer-Verlag, "Dynamics of Quiescent Prominences" IAU Colloquium, 117), 363, 1
Matsuno K. and Hirayama T., 1988, Solar Phys., 117, 21
Mein P., 1977, Solar Phys., 54, 55
Mein P., Mein N., 1982, Solar Phys., 80, 161
Parker, E. N., 1978, ApJ, 221, 238
Pikel'ner S. B., 1969, AZh, 46, 328
Schmieder B., Vial, J. C., Mein, P., Tandberg-Hanssen E.: 1983, A&A, 127, 337
Schmieder B., Raadu M. A. and Wiik J. E., 1991, A&A, 252, 353
Steinitz R., Gebbie K. B., Bar V., 1977, ApJ, 213, 269
Tsiropoula G., Georgakilas A.A., Alissandrakis C. E. and Mein P., 1992, A&A, 262,587
Vernazza J.E., Avrett E.H. and Loeser R., 1981, ApJSS, 45, 635

This article was processed by the author using Springer-Verlag LaTeX A&A style file version 3.